Automated methodology to locate notches with Lamb waves

Stefan Hurlebaus
Institute A of Mechanics
University of Stuttgart, Allmandring 5 b, D-70550 Stuttgart, Germany
s.hurlebaus@mecha.uni-stuttgart.de

Marc Niethammer, Laurence J. Jacobs
School of Civil and Environmental Engineering,
Georgia Institute of Technology, Atlanta, Georgia 30332-0355
mn@kyb.uni-stuttgart.de, laurence.jacobs@ce.gatech.edu

Christine Valle
Department of Mechanical Engineering,
University of Maine, Orono, ME 04469-5711
valle@umeme.maine.edu

Abstract: This study develops an automated method capable of detecting notches in isotropic plates. Laser ultrasonic techniques are used to generate and detect Lamb waves in perfect and notched plates. These signals are first transformed into the time-frequency domain using a short time Fourier transform (STFT) and subsequently into the group velocity-frequency domain. Finally, the notch is located with an autocorrelation in the group velocity-frequency domain. A verification of the proposed methodology shows excellent agreement with the actual location of the notch.

PACS number: 43.20.Mv, 43.35.Cg
Date Received: April 19, 2001 **Date Accepted:** May 20, 2001

1. Introduction

This research develops an automated methodology using time-frequency representations (TFRs) to locate notches in plates. This technique is based on the feasibility of calculating a group velocity-frequency representation from a TFR, as well as the invariance of the group velocity-frequency spectrum with respect to propagation distance.

Previous researchers have used Lamb waves for material characterization (see Chimenti[1] for details), but a Lamb wave's multi-mode and dispersive nature makes interpretation of time-domain signals difficult. In contrast, TFRs operate on time-domain signals, are capable of resolving a plate's individual modes, and naturally lead to the group velocity-frequency representation. TFRs are well-known in the signal processing community (see Cohen[2] for a review of TFRs). Previous research has shown that TFRs based on the short time Fourier transform (STFT) – spectrogram, reassigned spectrogram[3] – and the (pseudo) Wigner-Ville distribution[4] are particularly well suited for representing Lamb waves. These particular TFRs are effective in this application because of their constant time-frequency resolution over all times and frequencies.[3] Lemistre *et al.*[5] and Wilcox *et al.*[6] used the TFRs of Lamb waves for damage detection in composite plates.

The current study considers broadband, laser-generated, and detected Lamb waves in both perfect and notched plates. The notch is located by isolating the contributions of the signal reflected from this discontinuity by performing an autocorrelation of a series of group velocity spectra, each calculated with different, assumed propagation distances. Finally, note that the high-fidelity, broad-bandwidth, and noncontact nature of laser ultrasonics are critical elements for the success of this research.

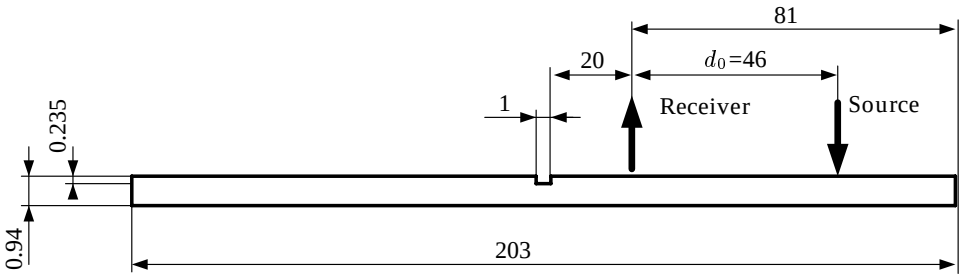

Fig. 1: Geometry of the notched plate with source and receiver locations (dimensions in mm).

2. Time-frequency representation

The experimental procedure makes resonance-free measurements of Lamb waves over a wide frequency range (200 kHz to 10 MHz). Broadband Lamb waves are generated with a Nd:YAG laser source (see Scruby and Drain[7] for details on laser ultrasonics). Laser detection of these waves is accomplished with a heterodyne interferometric receiver[8] that uses the Doppler shift to measure out-of-plane surface velocity (particle velocity) at a point on the plate's surface. Figure 1 shows the 0.94 mm thick 3003 aluminum plate (203 mm in length and 153 mm in width) used in this study, plus the relative locations of the laser source and receiver. One plate does not contain a notch (perfect plate specimen) whereas the second plate contains a notch in the middle of the plate (at 101.5 mm) with a notch depth of 0.235 mm and a notch width of 1 mm (notched plate specimen). The notch-receiver and the source-receiver (d_0) distances are 20 and 46 mm, respectively, for all results presented. Figure 2 (left) shows a time-domain signal measured in the notched plate specimen. The Nd:YAG laser fires at $t = 0$ and generates a Lamb wave at the source location. Note that all signals are discretized with a sampling frequency of 100 MHz, low-pass filtered at 10 MHz, and represent an average of twenty Nd:YAG shots to increase the signal-to-noise ratio.

This time-domain signal is transformed into the time-frequency domain using the STFT, essentially chopping the signal into a series of small overlapping pieces. Each of these pieces is windowed and then individually Fourier transformed. The energy density spectrum of a STFT is called a spectrogram.[2] Figure 2 (right) shows the contour plot of the square root of the spectrogram of the time-domain signal (the left of Fig. 2), using a 384-point long Hanning window. The TFR of Fig. 2 (right) is rather complicated, containing both incident and reflected (from the notch and edges) contributions. Figure 2 contains an excellent representation of the incident Lamb modes (see [3] for details), but it is difficult to quantitatively identify the individual reflected contributions. One possible technique to identify the reflected modes in Fig. 2 would be to visually compare Fig. 2 with its perfect, infinite plate counterpart. Unfortunately, the Lamb wave's multiple modes plus the finite time-frequency bands present in Fig. 2 (these finite bands are present because of the Heisenberg uncertainty principle[3]) make it difficult to develop a quantitative, visual comparison. As an alternative to a visual approach, consider a more objective methodology that uses an autocorrelation in the group velocity-frequency domain.

3. Group velocity-frequency representation and correlation

The TFR in Fig. 2 can be transformed into the group velocity-frequency domain using

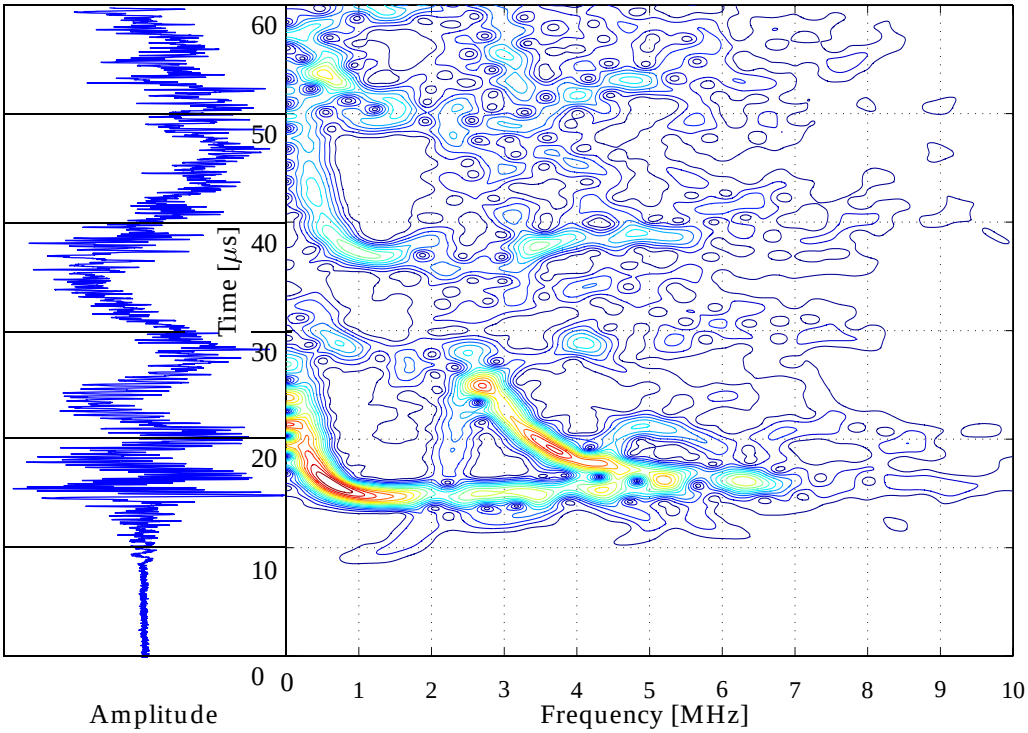

Fig. 2: Time- and time-frequency-domain signal measured in the notched plate.

the relationship $c_{gr} = d/t$, where c_{gr} is the group velocity, d is the propagation distance, and t is the propagation time (for each frequency). However, this transformation is complicated by any reflected contributions contained in a signal — the modes reflected from a notch or an edge will have different propagation distances, *d*, than the incident's source-receiver distance, d_0 in Fig. 1. Fortunately, the incident and reflected contributions all propagate within the same plate, so they should have the same group velocity-frequency spectrum — except for any mode conversion (portions of certain modes might appear or disappear from incidence to reflection). This feature plus the group velocity-frequency representation's invariance to propagation distance are exploited to calculate the unknown notch-receiver distance.

First, determine the group velocity-frequency representation for the incident modes by calculating c_{gr} with the *known* source-receiver distance; Fig. 3 shows the group velocity of the incident modes obtained by transforming Fig. 2 with $d = d_0$. The theoretical values of the Rayleigh-Lamb spectrum of the corresponding infinite, perfect plate are included in Fig. 3 as solid lines for visualization purposes only. There is excellent agreement between the incident modes (above 1800 m/s) and the theoretical dispersion curves, whereas there are modes with group velocities below 1600 m/s that do not correspond to any of the theoretical modes. These group velocities are spurious artifacts of the reflected modes, since the group velocity-frequency spectrum of Fig. 3 is only valid for the incident modes. The incident modes have a propagation distance equal to the source-receiver distance (d_0), although the reflected modes have traveled different (unknown) propagation distances. Finally, note that there are no group velocities below $c_{gr} = 750$ m/s because time is finite in the time domain signal.

The contributions of reflected modes are isolated by calculating a new group velocity-frequency representation of the *same* time-domain signal, but with a new prop-

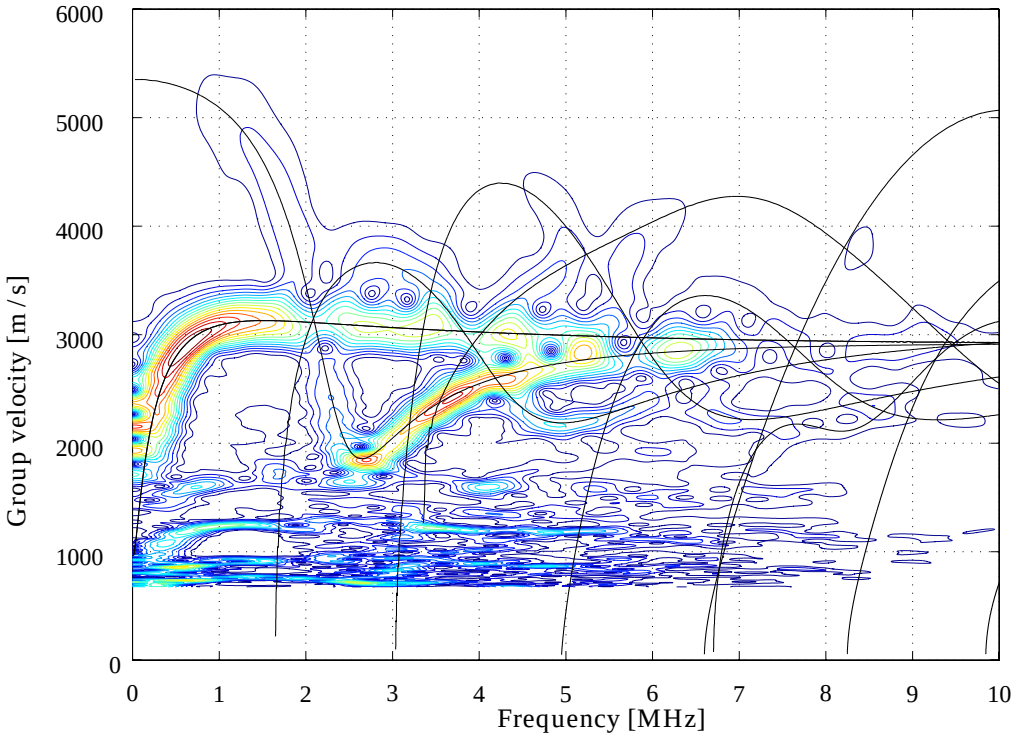

Fig. 3: Group velocity-frequency representation of the notched plate calculated with d as the source-receiver distance, d_0 (exact for incident modes).

agation distance equal to $d = d_0 + 2\Delta d$, where Δd will be used to represent the *unknown* receiver-notch distance. For illustrative purposes, Fig. 4 uses the *exact* propagation distance from the source to the receiver plus twice the distance from the receiver to the notch ($d = d_0 + 2\Delta d = 46 + 2 \times 20 = 86$ mm) to transform Fig. 2. As is the case for Fig. 3, the solid lines in Fig. 4 are the theoretical spectrum of the corresponding infinite, perfect plate. The modes reflected from the notch (the exact propagation distance d used to calculate Fig. 4) should overlay the solid lines, and a portion of a reflected mode is barely visible around 3000 m/s. Note that the additional modes above 3000 m/s are the spurious artifacts of the incident modes, whereas the modes around 2400 m/s are artifacts of the signal reflected from the closest edge. Figure 4 demonstrates that it is extremely difficult to visually identify the reflected modes without the aid of the theoretical spectrum (the calculation of this spectrum is not trivial for more complicated specimen geometries or materials) plus a priori knowledge of the notch's location.

An objective, alternative approach (that does not rely on a theoretical spectrum) is to systematically vary the value of Δd (and the associated propagation distance $d = d_0 + 2\Delta d$) and calculate a new group velocity spectrum for each propagation distance. Next, autocorrelate each new group velocity-frequency spectrum with the group velocity-frequency spectrum of the same time-domain signal, but calculated with a propagation distance of d_0. Obviously, this autocorrelation reaches its maximum for a spectrum calculated with $\Delta d = 0$ (the correlation of two identical signals), but reflections will introduce local maxima in the correlation curve at certain Δd's. These local maxima occur when the reflected modes exactly coincide with any of the corresponding incident modes (in the group velocity-frequency spectrum) and are a measure of the receiver-reflector distance. Note that this exact coincidence occurs when the

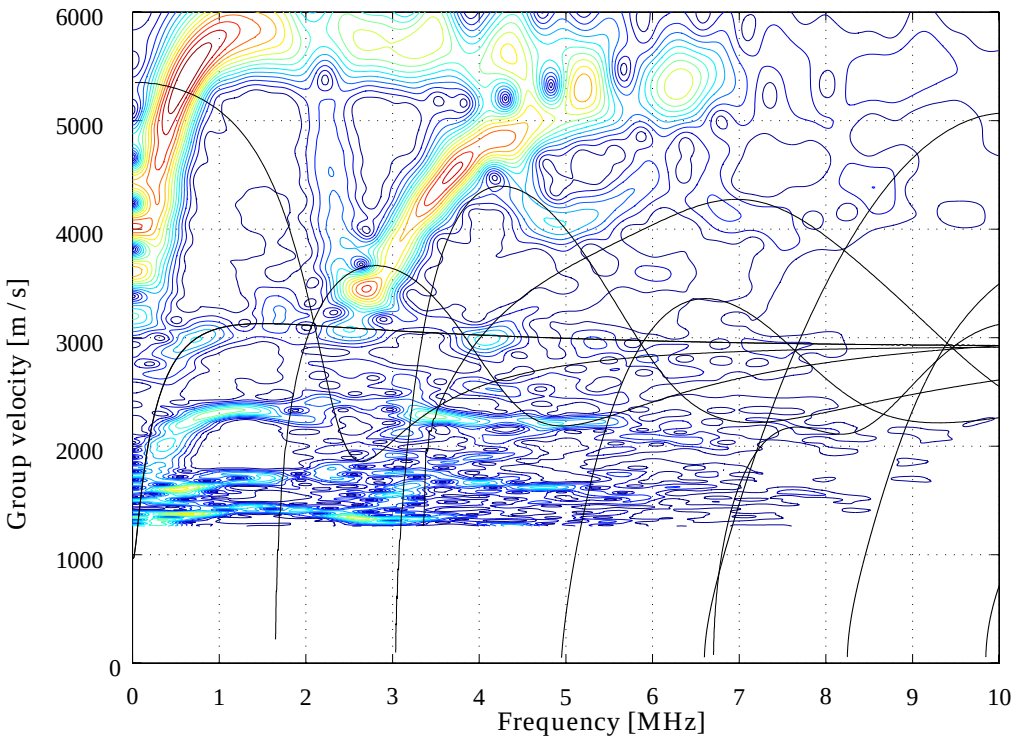

Fig. 4: Group velocity-frequency representation for the notched plate obtained with d as the source-receiver plus twice receiver-notch distance (exact for modes reflected from the notch).

modes reflected from the notch overlay the theoretical spectrum in Fig. 4 at Δd equal to the exact receiver-notch distance.

Figure 5 shows the correlation of the spectra of the perfect plate (green curve) for 301 values of Δd, varying from 0 to 60 mm with a increment step of 0.2 mm. Each of these spectra (calculated with a propagation distance $d = d_0 + 2\Delta d$) is correlated with the spectrum of the same perfect plate calculated with a propagation distance of $d = d_0$. This procedure is repeated for the notched plate specimen (correlated with the notched plate with $d = d_0$) and shown in Fig. 5 as the red curve. The correlation of the notched plate shows a local maximum at $\Delta d = 20$ mm that is not present in the perfect plate correlation, whereas both correlation curves show local maxima at $\Delta d = 35$ and 55 mm. The first maximum corresponds to the notch (in the notched plate), whereas the other two maxima correspond to the two closest edges (the edge for the 55 mm peak is in the width of the plate and is not shown in Fig. 1). For a further enhancement of any features that are present in the notched plate, but not in the perfect plate, the notched plate correlation curve is divided by the perfect plate correlation curve. The result, shown as the blue curve in Fig. 5, has a single dominant peak at $\Delta d = 20$ mm. This peak corresponds to the exact receiver-notch distance, shown in Fig. 1. Note that the accuracy of this "measurement" is $\pm 1\%$ for the discretization (sampling distance Δd) of 0.2 mm and all of the correlations are performed through a group velocity band of 1800–3500 m / s.

4. Conclusion

This note clearly demonstrates the effectiveness of using an autocorrelation of group velocity-frequency representations to develop an automated methodology to locate

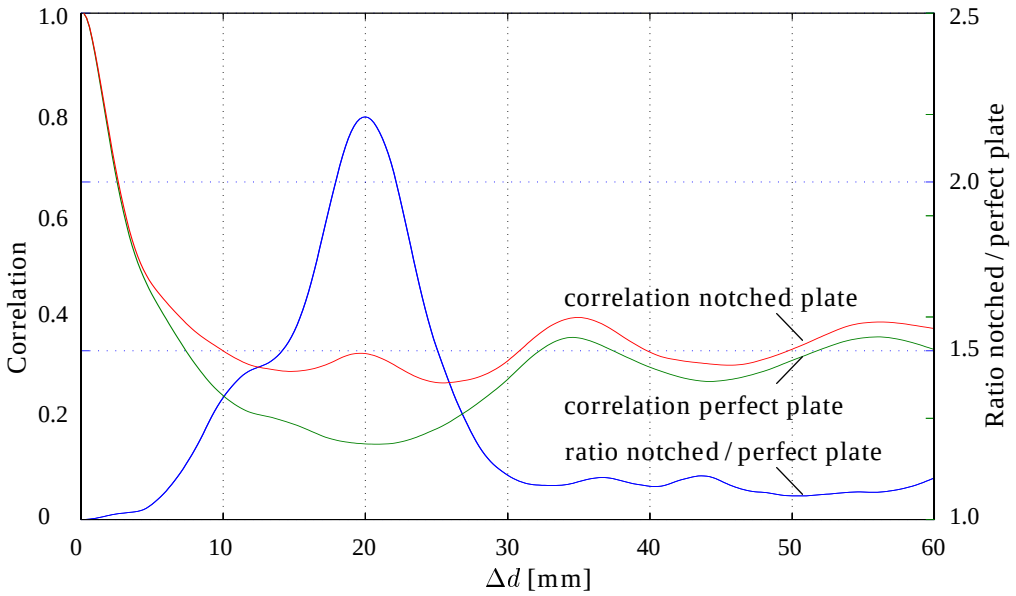

Fig. 5: Correlation curves for the perfect plate, notched plate, and a division of both curves.

notches with Lamb waves. This procedure exploits the invariance of the group velocity-frequency spectrum with respect to propagation distance to quantitatively isolate the modes reflected from a notch. The proposed procedure overcomes difficulties associated with the multi-mode and dispersive nature of Lamb waves, enabling the accurate calculation of propagation distances of reflected modes. Note that this research is restricted to one-dimensional localization of notches in isotropic plates, but it can be extended to more realistic defects (such as cracks), two-dimensional wave propagation in plates, or composite plates.

References

[1] D.E. Chimenti, "Guided waves in plates and their use in materials characterization," Appl. Mech. Review, **50(5)**, 247-284 (1997).
[2] L. Cohen, *Time-Frequency Analysis* (Prentice-Hall, New Jersey, 1995).
[3] M. Niethammer, L.J. Jacobs, J. Qu, and J. Jarzynski, "Time-frequency representations of Lamb waves," J. Acoust. Soc. Am., **109(5)**, 1841–1847 (2001).
[4] W.H. Prosser, M.D. Seale, and B.T. Smith, "Time-frequency analysis of the dispersion of Lamb modes," J. Acoust. Soc. Am., **105**, 2669–2676 (1999).
[5] M. Lemistre, and D. Balageas, "Structural health monitoring based on diffracted Lamb waves analysis by discrete wavelet transform," in: *System Identification and Structural Health Monitoring*, edited by A. Guemes (Graficas, Madrid, 2000) pp. 561-569.
[6] P.D. Wilcox, R.P. Dalton, M.J.S. Lowe, and P. Cawley, "Mode selection and transduction for structural monitoring using Lamb waves" in: *Structural Health Monitoring 2000*, edited by F.-K. Chang (Technomics Publ., New York, 1999) pp. 703-712.
[7] C. B. Scruby, and L.E. Drain, *Laser Ultrasonics: Techniques and Applications* (Adam Hilger, Bristol, 1990).
[8] D.A. Bruttomesso, L.J. Jacobs, and R.D. Costley, "Development of an interferometer for acoustic emission testing," J. Eng. Mech., **119**, 2303–2316 (1993).